

学位論文

Gene expression changes in the retina
after systemic administration of
aldosterone

香川大学大学院医学系研究科
分子情報制御学専攻

小野 葵



Gene expression changes in the retina after systemic administration of aldosterone

Aoi Ono¹ · Kazuyuki Hirooka¹ · Yuki Nakano¹ · Eri Nitta¹ · Akira Nishiyama² · Akitaka Tsujikawa¹

Received: 1 May 2017 / Accepted: 2 April 2018
 © Japanese Ophthalmological Society 2018

Abstract

Purpose Retinal ganglion cell (RGC) loss associated with thinning of the retinal nerve fiber layer without elevated intraocular pressure (IOP) occurs after the systemic administration of aldosterone. Since it is important to determine the mechanism of cell death independent of the IOP, we examined gene expression changes in the retina after the systemic administration of aldosterone.

Methods Following subcutaneous implantation of an osmotic minipump into the mid-scapular region of rats, we administered an 80 µg/kg/day dose of aldosterone. Differences in the gene expression in the retina between normal rats and aldosterone-treated rats were investigated using microarrays. Real-time PCR was used to confirm the differential expression.

Results Analysis of the microarray data sets revealed the upregulation of 24 genes and the downregulation of 24 genes of key apoptosis-specific genes. Real-time PCR revealed 4 genes (*Cdknla*, *Tbox5*, *Pf4*, *Vdr*) were upregulated while 12 genes (*Acvr1c*, *Asns*, *Bard1*, *Card9*, *Crh*, *Fcgrla*, *Inhba*, *Kcnh8*, *Lck*, *Phldal*, *Ptprc*, *Sh3rf1*) were downregulated.

Conclusions Significant increases and decreases were noted in several genes after the systemic administration of aldosterone. Further studies will need to be undertaken in order to definitively clarify the role of these genes in the eyes of animals with normal-tension glaucoma.

Keywords Aldosterone · Retinal ganglion cell · Microarray · Retina · Glaucoma

Introduction

In normal-tension glaucoma (NTG), patients exhibit glaucomatous cupping of the optic nerve head with visual field damage even though there is an absence of elevated intraocular pressure (IOP) [1, 2]. In most patients with all other types of glaucoma, however, the IOP is reported to be a risk factor [3–6]. Although reduction of IOP prevents disease progression in most patients with NTG [7], in some there is still disease progression in spite of the reduction in IOP [8]. It is suggested that factors other than an elevated IOP might be involved in the progression of glaucoma [9]. Therefore, detailed evaluation needs to be conducted of the

new therapeutic approaches designed to treat this debilitating disease.

The systemic renin-angiotensin-aldosterone system (RAAS) plays an important role in both blood pressure and electrolyte homeostasis. Aldosterone, a steroid hormone, exerts its effects after it binds to a mineralocorticoid receptor (MR). Aldosterone causes an increase in reactive oxygen species (ROS) that subsequently activates NADPH oxidase and promotes inflammation [10, 11]. Compared to patients with essential hypertension, patients with primary aldosteronism have been shown to have a higher incidence of left ventricular hypertrophy [12], albuminuria [13], and stroke [14, 15]. Data from experimental animal studies demonstrate that aldosterone may play a role in mediating cardiovascular injury in the kidney and brain [14, 15]. Beneficial effects in the retina against ischemia-reperfusion injury are also reported after blockade of the angiotensin II type 1 receptor (AT1-R) and MR [16–18]. Moreover, within the retina there is considerable evidence that shows that all the components of the RAAS are expressed [19, 20]. In our previous experiments, we demonstrated that intravitreal injection of

✉ Aoi Ono
 aoiono@med.kagawa-u.ac.jp

¹ Department of Ophthalmology, Kagawa University Faculty of Medicine, 1750-1 Ikenobe, Miki, Kagawa 761-0793, Japan

² Department of Pharmacology, Kagawa University Faculty of Medicine, 1750-1 Ikenobe, Miki, Kagawa 761-0793, Japan

aldosterone reduced the number of RGCs [18], and more recently, we reported that, following the systemic administration of aldosterone there was a decrease in the number of RGCs without an elevation in the IOP and that, in addition, the administration of an MR blocker prevented RGC loss [20]. At the same time, the other cell layers appeared to be unaffected [18, 21].

At present the mechanism of cell death in this particular animal model remains unknown. The purpose of our current study was to investigate gene expression changes in the retina after the systemic administration of aldosterone.

Material and methods

Animals

Male Sprague-Dawley rats were obtained from Charles River Japan. The rats, which weighed 200 to 250 g, were permitted free access to standard rat food (Oriental Yeast Co., Ltd.) and tap water. All experiments were conducted in accordance with the approved animal care and standard guidelines for animal experimentation of the Kagawa University Faculty of Medicine. All the experiments adhered to the ARVO Statement for the Use of Animals in Ophthalmic and Vision Research. Approval at our ethics committee was not deemed necessary.

Experimental animals

Subcutaneous osmotic minipumps (Alzet model 2006, DURECT Corporation), which were implanted subcutaneously into the mid-scapular region of the rats, were used to administer an 80 µg/kg/day dose of aldosterone (Sigma-Aldrich). At 7 days after the systemic administration with or without aldosterone, the rats were sacrificed by administering an overdose of pentobarbital sodium. After the eyes were enucleated, the retinae were carefully isolated.

Histological examination

For the histological examination, rats were anesthetized by intraperitoneal injection of pentobarbital sodium (50 mg/kg) at 6 weeks after the systemic administration of aldosterone and then perfused intracardially with phosphate-buffered saline (PBS), followed by perfusion with 4% paraformaldehyde in PBS. Subsequently, the anterior segments, including the lens, were removed. The posterior eyecups were then embedded in paraffin, and thin sections (5-µm thickness) were cut using a microtome. Each of the sections was carefully cut to include the full length from the superior to inferior along the vertical meridian through the optic nerve head. Each eye was then mounted on a silane-coated glass slide

and stained with hematoxylin and eosin (HE). A microscopic image (Olympus BX-51, Olympus Inc.) of each section within 0.5 to 1 mm superior of the optic disc was scanned.

Microarray analysis

The microarray analysis examined a total of 7 controls and 7 treatment eyes. Each sample consisted of the retinal fraction from 7 eyes. The RNeasy mini Kit protocol (QIAGEN, GmBH) was used for the extraction of the total RNA. RNA sample integrity was verified through the use of a UV adsorption measurement and bioanalyzer. After using the Low Input Quick Amp Labeling Kit (Agilent Technologies) to amplify, label and purify the total RNA, the qualified total RNA was then further purified by the RNeasy mini spin column (QIAGEN). Subsequently, the qualified total RNA was further purified by Low Input Quick Amp Labeling Kit. Next, the array was washed by Agilent's Gene Expression Wash Buffer kit (Agilent Technologies). In the final step, the array slides were scanned by an Agilent Technologies Microarray Scanner (Agilent Technologies). Using the Agilent Feature Extraction 10.7.3.1, the same spot was quantified on each slide. Normalization of the raw data was performed as follows: importation of the scanned data to the GeneSpring GX 7.3.1, after which the data was processed and normalized to the 75 percentile.

Real-time PCR

Real-time PCR using a LightCycler FastStart DNA Master SYBR Green I kit and an ABI Prism 7000 Sequence Detection System (Applied Biosystems) were used to analyze the mRNA expression of GAPDH, and up- or downregulated genes in microarray analysis, as previously described [22, 23]. Briefly, after denaturation of the cDNA at 95°C for 30 s, it was then amplified by PCR for 45 cycles (95°C for 15 s followed by 60°C for 40 s). Table 1 lists the oligonucleotide primer sequences. After normalization of the GAPDH expression, all the data were expressed as relative differences.

In situ hybridization

We investigated gene expression site of Cdkn1a, Vdr and Pf4 by *in situ* hybridization. *In situ* hybridization was performed using ViewRNA™ ISH Tissue Assay (Affymetrix) following the manufacturer's protocol. Tissues were fixed for 24 hours at 4°C with paraformaldehyde solution (4% paraformaldehyde in phosphate buffer saline). FFPE tissues were sectioned at 4 micron and mounted on silane coated slides (Muto pure chemical co, ltd). Each of the sections was carefully cut to include the full length from the superior to inferior along the vertical meridian through the optic

Table 1 Primers for real time PCR

Gene	Sequence (5'-3')	Position	Size of production (bp)
Bcl3	Forward: CTGACAGCGGCCTCAAGAAC Reverse: AGAGGCCTTCCCTTAGGA	1021-1040 1112-1093	92
Fcgr2b	Forward: CTGTCGTCCATGTGCTCTCA Reverse: GTITCACCACAGCCTTCGGA	107-126 214-195	108
Htatip2	Forward: ATGGCGACAAGGAAACACT Reverse: GGCGCCAAAATAAAGACGG	12-31 89-70	78
Tbx5	Forward: TATIGTACCCGAGACGACC Reverse: ATAAAGGCAGCCGGCATAG	335-354 428-409	94
Acvr1	Forward: TGTGGAGTGTGCGGAAAG Reverse: ATGCCTCAGCATAACCGTGT	776-795 924-905	149
Alox15	Forward: GCCATCCAGCTTGAACCTCC Reverse: GGCTAGGAGCCAGTCCATTG	952-971 1038-1019	87
Birc3	Forward: GAAAAGGGAGGGGGAGGCC Reverse: CCTACGGAACCTTGCTGACCA	32-51 113-93	82
C-C motif	Forward: AGCCAACCTCTACTGAAGCC Reverse: AACTGTGAACAAACAGGCCA	34-53 117-96	84
C7	Forward: CCCAAGCATGAAGGCAACAAG Reverse: AAGGCCATAGGAGTCCCAC	134-154 246-227	113
Cdkn1a	Forward: TCCGCTCGGATTGTAAACCTC Reverse: GCACCAGCTTGGGATAGGG	1766-1786 1849-1830	84
Cdkn2c	Forward: TCTCGAGACGGATGGAAAG Reverse: ACAGTGGTACTGAGGCAG	443-462 513-494	71
Fosl1	Forward: CCACACTCCTGGCTTGTGA Reverse: TGGTITGGGCATGGGTATG	1034-1053 1146-1127	113
Il1rn	Forward: GATGGAAATCTGCAGGGGACC Reverse: GCATCTTGAGGGTCTTTCC	4-24 113-93	110
Lgals7	Forward: ATCCTCTAACGTGCGCTCAG Reverse: ACGATCTGACGAAACCCAC	350-369 465-446	116
Mael	Forward: GGCATGACCAAGCAACTGTG Reverse: TTCTGATGCCGCTCCATAC	648-667 787-768	140
Msx1	Forward: TTCCTCCTCCCTTCCGAC Reverse: TTGCATCCCCAGTTCCA	1194-1213 1316-1297	123
Myc	Forward: GGAAGGACTATCCAGCTGCC Reverse: TGGAGCATTCGGTTGTTG	1525-1544 1608-1589	84
Pf4	Forward: TGATCAAAGCAGGACCCAC Reverse: TACAGAGGTACTTGCCTGGTC	191-210 284-265	94
Snca	Forward: CAGCAGTCGCTCAGAAGACA Reverse: GTGGGTACCCCTTCTCACCC	388-407 489-470	102
Terc	Forward: GTCTTTGTCTCCGCCG Reverse: GCTGCAGGTCTGAACCTTCC	32-51 101-82	70
Txnip	Forward: CAAGTCTCCAGCCTCAAGGG Reverse: TTCCGACATTACCCAGCAA	1517-1536 1592-1573	76
Tnfrsf8	Forward: TGGGTCACTGACAGATTCCAG Reverse: TGGGAGCAAAGAGTTCCAG	1122-1142 1267-1247	146
Vegfa	Forward: ATTCAACGGACTCATCAGCCA Reverse: CCGTGGCAGGATITAAGAGG	96-116 231-211	136
Vdr	Forward: TGATCCAGAAACTGGCCGAC Reverse: GCTATTCTGGGCTGGAAGG	1230-1249 1315-1296	86
Adamts14	Forward: GACCTGAGGCGAATTCCCTG	83-102	88

Table 1 (continued)

	Gene	Sequence (5'-3')	Position	Size of production (bp)
		Reverse: TAGGAATCTGGCGCAAGCC	170-151	
	Bard1	Forward: TGAACACCACCGCTATCAC	1446-1465	145
		Reverse: TCTGTGTAATCCACTGGCG	1590-1571	
	Cd3 g	Forward: TGGAGTCGCCAGTCAAGAG	473-492	75
		Reverse: TCCTTGAGGGGCTGGTAGAC	547-528	
	Fcgr1a	Forward: GCTATTGCCCCACACCAGTGC	573-592	71
		Reverse: TCAGGATGACCAGACTCCCC	643-624	
	Gimap5	Forward: TGTGTCTGGGGATGTICA	26-45	127
		Reverse: ACTCGCAGAGCTGTAAACCC	152-133	
	Ndufaf4	Forward: CTGTACCGGTGGGTCTTGG	1361-1380	121
		Reverse: GCCTGGCCTTTGCCATITA	1481-1462	
	Sh3rf1	Forward: TACTCGCCTCTACACCGTCA	1229-1248	124
		Reverse: GGCGTAAATGTGCGATCTG	1352-1333	
	Acvr1c	Forward: TACCTGCCAACCGAAGGGAG	260-279	140
		Reverse: CGGTCTGGTCACGTTGTTG	399-380	
	Asns	Forward: AACCTGGAAAATTCGGCG	71-90	119
		Reverse: TGCCACACATGCTACAGGAG	189-170	
	Bdnf	Forward: CTICGGTTGCATGAAGGCTG	108-127	135
		Reverse: GTCAGACCTCTGAACCTGC	242-223	
	Cdh1	Forward: GCCCAGGAAATACACCCCCTC	3792-3811	75
		Reverse: ACTCAGGTCAAATCAGCCG	3866-3847	
	Casp7	Forward: AGGCCCTCTICAAGTGCTTC	285-304	84
		Reverse: GCAGATCCTGCATCTTGCG	368-349	
	Card9	Forward: GGATGAGAACTACGACCTGGC	649-669	142
		Reverse: CACCTIGCAGTCATCCTCTGC	790-770	
	C5ar1	Forward: TCTACTTGGCCGTGTTCTG	174-193	89
		Reverse: GGCCTTGACAGTACGTTGG	262-243	
	C6	Forward: TCAGATGCTTACAGACAGAAC	2053-2075	150
		Reverse: TGGGACAGGTCAGCTCAATG	2202-2183	
	Crh	Forward: GCAACCTCAGCCGATCTGA	325-344	77
		Reverse: CAGCGGGACTTCTGTTGAGG	401-382	
	Cryaa	Forward: GGCTCCTGCCTGACTCATTG	7-26	71
		Reverse: CTGGATGGTGACGTCCATGT	77-58	
	Inhba	Forward: CCCAGTGTCTAGCAGCATCC	833-852	71
		Reverse: CACAAGCAATCCGCACATCC	903-884	
	Phlda1	Forward: GAACCGTCCCAACCTAGTGG	623-642	116
		Reverse: TATACTTGCCTTGCCTCC	740-721	
	Kcnh8	Forward: GTACTACGGCAACAAACACGC	1267-1286	128
		Reverse: TCTCTGCATCCGTGTTAGCG	1394-1375	
	Ptprc	Forward: TTGCTCCCCATCCGATAAGAC	44-64	108
		Reverse: AGCTGAAGGCCAGAAGTTGA	151-131	
	Ripk3	Forward: AGTCAGGGAAATCAAGCCTTA	126-146	125
		Reverse: CCTCTTGTGGGTCTGGATG	250-231	
	Lck	Forward: CGATCTGGTCCGCCATTACA	617-636	89
		Reverse: ATGGTTCTGGGGCTCTGG	705-686	
	ERbb3	Forward: CTGGGAGAATGCTTGGCAGA	1606-1625	111
		Reverse: TTCCCGGCTGTAGTTTCGAC	1716-1697	

nerve head. Rat *Cdkn1a*-gene-specific probe (Accession No. NM_080782.3), Rat *Pf4*-gene-specific probe (Accession No. NM_001007729.1) and Rat *Vdr*-gene-specific probe (Accession No. NM_017058.1) were designed and synthesized by Affymetrix. A no-probe sample was utilized as a negative control. Nuclei were stained for 5 min with Hoechst 33342 (Sigma-Aldrich) and samples were Dako Ultramount (Dako). Hybridized target mRNAs were visualized using fluorescent microscopy (BZ-X700, KEYENCE) and observed in 4 points in each slides, 1 mm (central) and 4 mm (peripheral) away from the optic disc.

Statistical analysis

All data were analyzed using Wilcoxon signed-rank test, with the data then presented as the mean \pm SD. Statistical analyses were performed using SPSS version 19.0 (SPSS Inc., Chicago, IL). A *P* value of less than 0.05 was considered statistically significant.

Results

Histological examination of RGC loss

Aldosteron-treated rats showed a neuronal loss in the ganglion cell layer (Fig. 1).

Microarray analysis of gene expression

After systemic administration of aldosterone, we used microarray analysis to determine the gene expression changes in the retina. The changes in the level of expression of the genes (upregulated or downregulated by > 2.0 -fold versus baseline) were then compared between the naïve rats

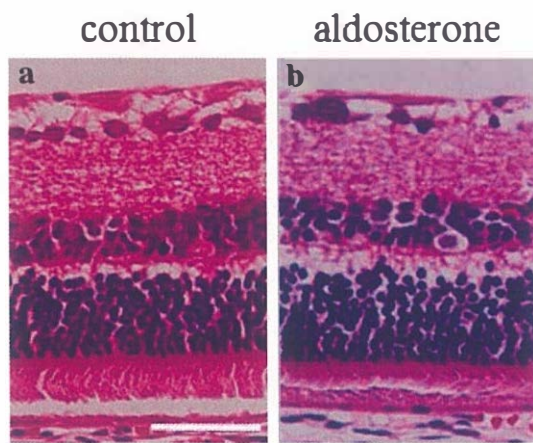


Fig. 1 Light micrographs of the retina of an eye treated with 80 µg/kg/day aldosterone for 2 weeks and a normal control eye. Scale bar, 50 µm

(baseline: day 0) and the rats on day 7 after the systemic administration. The gene expression changes' observed in the retina at 1 week after systemic administration of aldosterone are summarized in Table 2, with 24 genes found to be either up- or downregulated in each cluster.

Ratio of RNA expression

Table 3 shows the ratio of RNA expression of protein specific RGC and other retinal neurons based on the microarray analysis. There was no significant change in either gene.

mRNA levels after systemic administration of aldosterone

Real-time PCR technique was used to measure the mRNA levels of the 48 genes that had been detected by

Table 2 Results of microarray assay

Up regulation	Ratio	Down regulation	Ratio
<i>Acvr1</i>	2.028	<i>Acvr1c</i>	0.384
<i>Alox15</i>	11.059	<i>Adamtsl4</i>	0.489
<i>Birc3</i>	13.423	<i>Asns</i>	0.224
<i>Bcl3</i>	9.804	<i>Bard1</i>	0.386
<i>C7</i>	2.454	<i>Bdnf</i>	0.364
<i>C-C motif</i>	7.972	<i>Card9</i>	0.199
<i>Cdkn1a</i>	3.071	<i>C5ar1</i>	0.168
<i>Cdkn2c</i>	2.031	<i>C6</i>	0.424
<i>Fcgr2b</i>	3.092	<i>Casp7</i>	0.385
<i>Fosl1</i>	13.808	<i>Cd3g</i>	0.443
<i>Htr1tp2</i>	6.056	<i>Cdh1</i>	0.273
<i>Illrn</i>	2.527	<i>Crh</i>	0.374
<i>Tnfrsf8</i>	17.7	<i>Cryaa</i>	0.473
<i>Txnip</i>	3.764	<i>Erbb3</i>	0.298
<i>Vegfa</i>	2.315	<i>Fcgr1a</i>	0.482
<i>Vdr</i>	2.003	<i>Gimap5</i>	0.372
<i>Lgals7</i>	2.973	<i>Inhba</i>	0.488
<i>Mael</i>	5.791	<i>Kcnh8</i>	0.12
<i>Msx1</i>	2.034	<i>Lck</i>	0.206
<i>Myc</i>	2.234	<i>Ndufaf4</i>	0.141
<i>Pf4</i>	2.545	<i>Phlda1</i>	0.444
<i>Snca</i>	48.514	<i>Ptprc</i>	0.466
<i>Tbx5</i>	14.656	<i>Ripk3</i>	0.443
<i>Terc</i>	2.766	<i>Sh3rf1</i>	0.048

Table 3 Ratio of RNA

Gene	Ratio
<i>Pax6</i>	1.189
<i>Thy1</i>	1.051
<i>Rho</i>	1.024

the microarray. Although the microarray analysis showed there was upregulation of *Acvr1*, *Alox15*, *Cdkn2c*, *Il1rn*, *Snca*, *Terc* and *Vegfa*, RT-PCR showed that these genes were downregulated. When compared to the normal retina, there were 4 genes (*Cdknla*, *Pf4*, *Tbx5*, and *Vdr*) (Table 4) that exhibited upregulated mRNA levels after the systemic administration of aldosterone, while 12 gene expressions exhibited downregulated levels (*Acvr1c*, *Asns*, *Bard1*, *Card9*, *Crh*, *Fcgrla*, *Inhba*, *Kcnh8*, *Lck*, *Phldal*, *Ptprc*, and *Sh3rf1*) (Table 5).

Expression of mRNA in the retina

Expression of *Cdknla*, *Vdr* and *Pf4* was examined using *in situ* hybridization (Fig. 2). *Cdknla* was widely observed in the retina. In particular, strong *Cdknla* expression was observed in the ganglion cell layer (GCL). *Vdr* and *Pf4* expression were observed in the outer plexiform layer (OPL) and in the outer nuclear layer (ONL). In addition, weak expression of *Vdr* was observed in the inner plexiform layer (IPL) and in the inner nuclear layer (INL).

Table 4 Results of real time PCR for upregulated genes

Gene	Control (n=10) Mean±SD	Aldosterone (n=10) Mean±SD	P-value
<i>Acvr1</i>	0.732±0.089	0.598±0.059	0.028*
<i>Alox15</i>	0.755±0.260	0.486±0.363	0.028*
<i>Bcl3</i>	0.779±0.121	0.963±0.449	0.386
<i>Birc3</i>	0.609±0.074	0.655±0.113	0.284
<i>C7</i>	1.237±0.276	1.046±0.125	0.169
<i>C-C motif</i>	0.936±0.208	0.896±0.179	0.959
<i>Cdkn1a</i>	0.958±0.183	1.661±0.474	0.012*
<i>Cdkn2c</i>	0.790±0.161	0.603±0.082	0.028*
<i>Fcgr2b</i>	1.098±0.190	1.141±0.266	0.575
<i>Fosl1</i>	0.740±0.231	0.728±0.143	0.721
<i>Htatip2</i>	0.452±0.089	0.497±0.227	0.959
<i>Il1rn</i>	3.615±1.765	1.473±0.900	0.005*
<i>Lgals7</i>	1.409±0.693	0.948±0.130	0.092
<i>Mael</i>	0.551±0.343	0.552±0.119	0.799
<i>Msx1</i>	0.586±0.185	0.662±0.278	0.386
<i>Myc</i>	0.794±0.104	0.756±0.161	0.444
<i>Pf4</i>	0.589±0.108	0.990±0.247	0.005*
<i>Snca</i>	1.052±0.097	0.751±0.066	0.005*
<i>Tbx5</i>	0.688±0.363	0.862±0.080	0.005*
<i>Terc</i>	1.073±0.050	0.871±0.165	0.004*
<i>Tnfrsf8</i>	0.624±0.318	0.869±0.247	0.070
<i>Txnip</i>	0.788±0.098	0.682±0.351	0.382
<i>Vegfa</i>	0.988±0.127	0.646±0.097	<0.001*
<i>Vdr</i>	0.950±0.183	1.130±0.193	0.046*

SD standard deviation, *P<0.05, Wilcoxon signed-rank test

Table 5 Results of real time PCR for downregulated genes

Gene	Control (n=10) Mean±SD	Aldosterone (n=10) Mean±SD	P-value
<i>Acvr1c</i>	2.591±4.875	0.653±0.162	0.005*
<i>Adamtsl4</i>	0.810±0.177	1.012±0.263	0.092
<i>Asns</i>	0.925±0.159	0.201±0.043	0.005*
<i>Bard1</i>	0.625±0.157	0.469±0.058	0.028*
<i>Bdnf</i>	1.004±0.098	1.006±0.124	0.959
<i>Card9</i>	0.862±0.112	0.771±0.038	0.012*
<i>C5ar1</i>	0.872±0.160	0.973±0.270	0.114
<i>C6</i>	0.461±0.182	0.611±0.217	0.114
<i>Casp7</i>	0.887±0.037	0.869±0.187	0.444
<i>Cd3 g</i>	0.481±0.129	0.389±0.152	0.241
<i>Cdh1</i>	0.512±0.244	0.464±0.070	0.878
<i>Crh</i>	2.482±3.993	0.784±0.102	0.005*
<i>Cryaa</i>	0.521±0.295	0.498±0.214	0.721
<i>Erbb3</i>	0.528±0.369	0.350±0.181	0.284
<i>Fcgrla</i>	0.520±0.201	0.323±0.095	0.005*
<i>Gimap5</i>	0.588±0.289	0.504±0.060	0.444
<i>Inhba</i>	0.749±0.131	0.644±0.045	0.007*
<i>Kcnh8</i>	0.794±0.205	0.504±0.084	0.005*
<i>Lck</i>	0.785±0.168	0.636±0.094	0.028*
<i>Ndufaf4</i>	0.572±0.273	0.432±0.057	0.114
<i>Phldal</i>	0.956±0.218	0.644±0.198	0.037*
<i>Ptprc</i>	0.794±0.164	0.494±0.103	0.007*
<i>Ripk3</i>	0.621±0.174	0.793±0.367	0.241
<i>Sh3rf1</i>	0.788±0.257	0.575±0.104	0.012*

SD standard deviation, *P<0.05, Wilcoxon signed-rank test

Discussion

The current study showed that apoptosis was associated with the systemic administration of aldosterone, with 4 genes exhibiting upregulation and 12 genes showing downregulation. Since our previous study demonstrated there was a significant decrease in RGCs at 2 weeks after the continual administration of aldosterone [21], the present study investigated the changes in the gene expression in the retina at 1 week after administration, at a point prior to the death of the RGCs.

In our previous work, we showed that the local aldosterone/MR system that exists in the retina can be modulated by the RAAS both dependently and independently [18]. Moreover, we also demonstrated that there was an increase in the expression of AT1-R at 12 hours after reperfusion [16, 17] and that the ROS production after 12 hours of ischemia-reperfusion was mediated via the NADPH oxidase pathway [17]. Thus, these results suggest that the ROS production via the local RAAS might be responsible for the retinal ischemic injury. Furthermore, our findings also suggested that the RGC death observed in aldosterone-treated rats might have

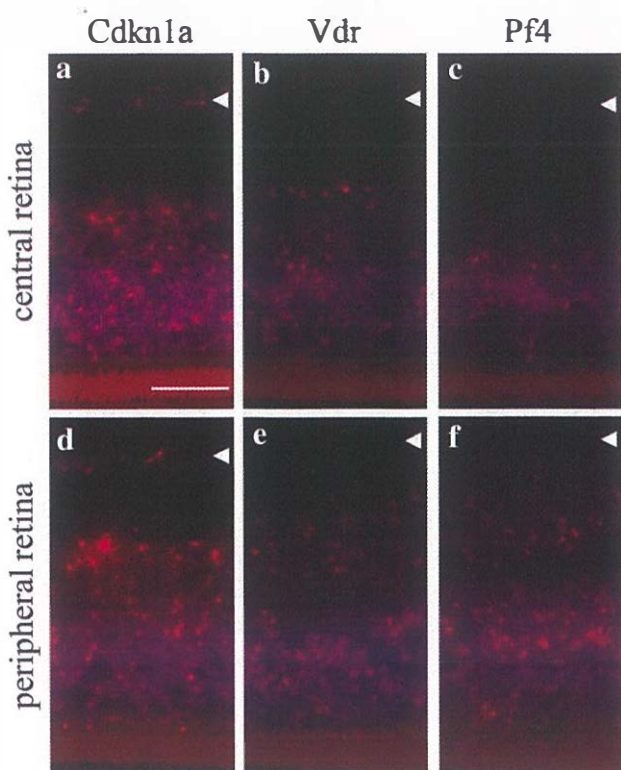


Fig. 2 Expression of Cdkn1a, Vdr or Pf4 in the retina. Fluorescent micrographs of in situ hybridization. Cdkn1a, (a) central and (d) peripheral retina. Vdr, (b) central and (e) peripheral retina. Pf4, (c) central and (f) peripheral retina. Micrographs of the central and peripheral areas were taken approximately 1 and 4 mm away from the optic nerve head. Scale bar, 50 μ m. Arrow head shows ganglion cell layer (GCL)

been induced by aldosterone in a ROS-dependent manner via a NADPH oxidase pathway. Based on these findings, we further explored the relationship between 15 genes and the NADPH oxidase pathway. Our results indicate that Cdkn1a, Pf4 and Vdr are associated with cell death via a NADPH oxidase pathway. However, RT-PCR showed that Acvr1, Alox15, Cdkn2c, IIrrn, Snca, Terc and Vegfa were downregulated while microarray analysis indicated that these genes were upregulated. Since microarray is a global gene analysis, false positive genes are sometimes observed. Another possible explanation of this discrepancy is that it is impossible to deny a cross reaction. Based on these findings, we decided not to further pursue the analysis of these 6 genes.

Platelet factor 4 (Pf4) activated monocytes are responsible for a long-lasting release of ROS that can selectively induce apoptosis in the endothelial cells [24]. This causes programmed cell death in endothelial cells, as inhibitors of the NADPH oxidase effectively blocked Pf4-induced monocyte oxidative burst and protected endothelial cells from undergoing apoptosis [24]. There are a number of soluble factors released by endothelial cells that can regulate

vascular tone and blood flow, including nitric oxide [25, 26]. Previous studies in animals and humans show that the inhibition of nitric oxide synthase reduces the blood flow [27, 28]. If there is an upregulation of Pf4, it is expected to reduce the blood flow. Thus, although in our current study we did not investigate the blood flow in the aldosterone-treated rats, these previous findings suggest that a reduced blood flow could have contributed to the RGC death in our animals. In fact, other studies that examined the retina and optic nerve head of glaucoma patients report finding reduced blood flow in these subjects [29, 30].

One of the important cyclin-dependent kinase inhibitors that induce cell cycle arrest is the cyclin-dependent kinase inhibitor 1A (CDKN1A), which is also referred to as p21. Since this kinase inhibitor can inhibit cell proliferation, it was initially thought that it could be used as a tumor suppressor [31, 32]. After damage to a cell, p53 will directly bind to the CDKN1A locus. Subsequently, it then activates the transcription of CDKN1A, PANDA and LincRNA-p21. p21 is able to mediate gene silencing by recruiting hnRPK, which then promotes apoptosis. Previous studies have examined p53 and demonstrate its ability to promote apoptosis. This is accomplished by transcriptionally activating or by repressing the expression of a panel of pro- and anti-apoptotic proteins [33]. Shi et al. [34] examined aldosterone-induced mesangial cell apoptosis and report that it caused the apoptosis via p53 both *in vitro* and *in vivo*.

Several studies report that depending upon the cell type and context, both the vitamin D receptor (VDR) and p53-signaling can regulate a variety of cellular functions involved in the development of cancer, including proliferation, differentiation, apoptosis and cell survival [35–37]. In addition, activators of the VDR have been shown to exhibit suppressant effects on the RAAS [38]. For example, activation of the VDR and the administration of losartan to block Ang II result in the inhibition of ROS generation [39]. However, none of the previous findings can explain why we found there was an upregulation of Vdr after the systemic administration of aldosterone.

Since our results indicate that Cdkn1a, Pf4 and Vdr were associated with cell death via a NADPH oxidase pathway, we investigated gene expression of Cdkn1a, Pf4 and Vdr using in site hybridization. Cdkn1a, but not Vdr or Pf4, signals were observed in GCL. This finding suggests that Cdkn1a may be associated with RGC death via a NADPH oxidase pathway.

MR is expressed in RGCs and in cells of the INL in the normal retina [19, 40]. So far, it is not clear why systemic administration of aldosterone causes only RGC loss, and not a loss of INL cells. Therefore, further investigation is needed to reveal why aldosterone causes only RGC loss.

The findings of our current study suggest there might be two possible mechanisms associated with the RGC death

that occurs after systemic administration of aldosterone. First, it is possible that ocular blood abnormalities due to the upregulation of PF4 could be involved in the death of the RGCs. Second, increases in the level of ROS might induce p53 activation as an upstream signal, thereby triggering the apoptosis. Further investigations are needed to clarify the mechanisms of RGC death after the systemic administration of aldosterone. We are currently performing additional studies designed to investigate the retinal blood flow after the systemic administration of aldosterone.

In conclusion, the systemic administration of aldosterone can lead to significant increases and decreases in various genes. Further functional studies on the effects of these genes are needed in order to definitively clarify the molecular mechanisms in the animal NTG model.

Acknowledgements This work was supported by a Grant-in-Aid for Scientific Research from the Ministry of Education, Culture, Sports, Science, and Technology of Japan (26462689).

Conflicts of interest A. Ono, None; K. Hirooka, None; Y. Nakano, None; E. Nitta, None; A. Nishiyama, None; A. Tsujikawa, Grant (Alcon, AMO Japan, Bayer, HOYA, Kowa, Novartis, Pfizer, Santen, Senju), Lecture fees (Alcon, AMO Japan, Bayer, Chugai, Kowa, Nidek, Novartis, Pfizer, Santen, Sanwa Kagaku, Senju).

References

- Levene RZ. Low tension glaucoma: a critical review and new material. *Surv Ophthalmol*. 1980;24:621–64.
- Quigley HA. Open-angle glaucoma. *N Engl J Med*. 1993;328:1097–106.
- Cartwright MJ, Anderson DR. Correlation of asymmetric damage with asymmetric intraocular pressure in normal-tension glaucoma (low-tension glaucoma). *Arch Ophthalmol*. 1988;106:898–900.
- Crichton A, Drance SM, Douglas GR, Schulzer M. Unequal intraocular pressure and its relation to asymmetric visual field defects in low-tension glaucoma. *Ophthalmology*. 1989;96:1312–4.
- Abedin S, Simmons RJ, Grant WM. Progressive low-tension glaucoma: treatment to stop glaucomatous cupping and field loss when these progress despite normal intraocular pressure. *Ophthalmology*. 1982;89:1–6.
- de Jong N, Greve EL, Hoyng PF, Geijssen HC. Results of a filtering procedure in low tension glaucoma. *Int Ophthalmol*. 1989;13:131–8.
- Oie S, Ishida K, Yamamoto T. Impact of intraocular pressure reduction on visual field progression in normal-tension glaucoma followed up over 15 years. *Jpn J Ophthalmol*. 2017. <https://doi.org/10.1007/s10384-017-0519-8>.
- Tezel G, Siegmund KD, Trinkaus K, Trinkaus K, Wax MB, Kass MA, et al. Clinical factors associated with progression of glaucomatous optic disc damage in treated patients. *Arch Ophthalmol*. 2001;119:813–8.
- Flammer J, Haefliger IO, Orgul S, Resink T. Vascular dysregulation: a principal risk factor for glaucomatous damage? *J Glaucoma*. 1999;8:212–9.
- Takebayashi K, Matsumoto S, Aso Y, Inukai T. Aldosterone blockade attenuates urinary monocyte chemoattractant protein-1 and oxidative stress in patients with type 2 diabetes complicated by diabetic nephropathy. *J Clin Endocrinol Metab*. 2006;91:2214–7.
- Shibata S, Nagase M, Yoshida S, Kawachi H, Fujita T. Podocyte as the target for aldosterone: roles of oxidative stress and Sgk1. *Hypertension*. 2007;49:355–64.
- Rossi GP, Sachetto A, Visentini P, Canali C, Graniero GR, Palatini P, et al. Changes in left ventricular anatomy and function in hypertension and primary aldosteronism. *Hypertension*. 1996;27:1039–45.
- Halimi J-M, Mimran A. Albuminuria in untreated patients with primary aldosteronism or essential hypertension. *J Hypertens*. 1995;13:1801–2.
- Takeda R, Matsubara T, Miyamori I, Hatakeyama H, Morise T. Vascular complications in patients with aldosterone producing adenoma in Japan: comparative study with essential hypertension. The Research Committee of Disorders of Adrenal Hormons in Japan. *J Endocrinol Invest*. 1995;18:370–3.
- Nishimura M, Uzu T, Fujii T, Kuroda S, Nakamura S, Inenaga T, et al. Cardiovascular complications in patients with primary aldosteronism. *Am J Kidney Dis*. 1999;33:261–6.
- Fukuda K, Hirooka K, Mizote M, Nakamura T, Itano T, Shiraga F. Neuroprotection against retinal ischemia-reperfusion injury by blocking the angiotensin II type 1 receptor. *Invest Ophthalmol Vis Sci*. 2010;51:3629–38.
- Fujita T, Hirooka K, Nakamura T, Itano T, Nishiyama A, Nagai Y, et al. Neuroprotective effects of angiotensin II type 1 receptor (AT1-R) blocker via modulating AT1-R signaling and decreased extracellular glutamate levels. *Invest Ophthalmol Vis Sci*. 2012;53:4099–110.
- Liu Y, Hirooka K, Nishiyama A, Lei B, Nakamura T, Itano T, et al. Activation of the aldosterone/mineralocorticoid receptor system and protective effects of mineralocorticoid receptor antagonism in retinal ischemia-reperfusion injury. *Exp Eye Res*. 2012;96:116–23.
- Wilkinson-Berka JL, Tan G, Jaworski K, Miller AG. Identification of a retinal aldosterone system and the protective effects of mineralocorticoid receptor antagonism on retinal vascular pathology. *Circ Res*. 2009;104:124–33.
- Wilkinson-Berka JL, Agrotis A, Deliyanti D. The retinal renin-angiotensin system: role of angiotensin II and aldosterone. *Peptides*. 2012;36:142–50.
- Nitta E, Hirooka K, Tenkomo K, Fujita T, Nishiyama A, Nakamura T, et al. Aldosterone: a mediator of retinal ganglion cell death and the potential role in the pathogenesis in normal-tension glaucoma. *Cell Death Dis*. 2013;4:e711.
- Rafiq K, Nakano D, Ihara G, Hitomi H, Fujisawa Y, Ohashi N, et al. Effects of mineralocorticoid receptor blockade on glucocorticoid-induced renal injury in adrenalectomized rats. *J Hypertens*. 2011;29:290–8.
- Rafiq K, Noma T, Fujisawa Y, Jshihara Y, Arai Y, Nabi AH, et al. Renal sympathetic denervation suppresses de novo podocyte injury and albuminuria in rats with aortic regurgitation. *Circulation*. 2012;125:1402–13.
- Woller G, Brandt E, Mittelstädt J, Rybakowski C, Petersen F. Platelet factor 4/CXCL4-stimulated human monocytes induce apoptosis in endothelial cells by the release of oxygen radicals. *J Leukoc Biol*. 2008;83:936–45.
- Cohen RA, Vanhoutte PM. Endothelium-dependent hyperpolarization: beyond nitric oxide and cyclic GMP. *Circulation*. 1995;92:3337–49.
- Ignarro LJ, Buga GM, Wood KS, Byrns RE, Chaudhuri G. Endothelium-derived relaxing factor produced and released from artery and vein is nitric oxide. *Proc Natl Acad Sci USA*. 1987;84:9265–9.

Gene expression changes in the retina after systemic administration of aldosterone

27. Luksch A, Polak K, Beier C. Effects of systemic NO synthase inhibition on choroidal and optic nerve head blood flow in healthy subjects. *Invest Ophthalmol Vis Sci.* 2000;41:3080–4.
28. Okuno T, Oku H, Sugiyama T, Yang Y, Ikeda T. Evidence that nitric oxide is involved in autoregulation in optic nerve head of rabbits. *Invest Ophthalmol Vis Sci.* 2002;43:784–9.
29. Yamazaki Y, Drance S. The relationship between progression of visual field defects and retrobulbar circulation in patients with glaucoma. *Am J Ophthalmol.* 1997;124:287–95.
30. Wang Y, Fawzi A, Varma R, Sadun AA, Zhang X, Tan O, et al. Pilot study of optical coherence tomography measurement of retinal blood flow in retinal and optic nerve diseases. *Invest Ophthalmol Vis Sci.* 2011;52:840–5.
31. Lehmann K, Tschauder C, Rickenbacher A, Jang JH, Oberkofer CE, Tschopp O, et al. Liver failure after extended hepatectomy in mice is mediated by a p21-dependent barrier to liver regeneration. *Gastroenterology.* 2012;143:1609–19.
32. Willenbring H, Sharma AD, Vogel A, Lee AY, Rothfuss A, Wang Z, et al. Loss of p21 permits carcinogenesis from chronically damaged liver and kidney epithelial cells despite unchecked apoptosis. *Cancer Cell.* 2008;14:59–67.
33. Wang DB, Kinoshita C, Kinoshita Y, Morrison RS. P53 and mitochondrial function in neurons. *Biochim et Biophys Acta.* 2014;1842:1186–97.
34. Shi H, Zhang A, He Y, Yang M, Gan W. Effect of p53 on aldosterone-induced mesangial cell apoptosis in vivo and in vitro. *Mol Med Rep.* 2016;13:5102–8.
35. Murray-Zmijewski F, Lane DP, Bourdon JC. p53/p63/p73 isoforms: an orchestra of isoforms to harmonise cell differentiation and response to stress. *Cell Death Differ.* 2006;13:962–72.
36. Vousden KH, Prives C. Blinded by the light: the growing complexity of p53. *Cell.* 2009;137:413–31.
37. Mason RS, Reichrath J. Sunlight vitamin D and skin cancer. *Anti-cancer Agents Med Chem.* 2013;13:83–97.
38. Husain K, Ferder L, Mizobuchi M, Finch J, Slatopolsky E. Combination therapy with paricalcitol and enalapril ameliorates cardiac oxidative injury in uremic rats. *Am J Nephrol.* 2009;29:465–72.
39. Rehman S, Chandel N, Salhan D, Rai P, Sharma B, Singh T, et al. Ethanol and vitamin D receptor in T cell apoptosis. *J Neuroimmune Pharmacol.* 2013;8:251–61.
40. Zhao M, Valamanesh F, Celerier I, Savoldelli M, Jonet L, Jeanny JC, et al. The neuroretina is a novel mineralocorticoid target: aldosterone up-regulates ion and water channels in Müller glial cells. *FASEB J.* 2010;24:3405–15.